Flora 233 (2017) 186–193

Contents lists available at ScienceDirect

Flora

journal homepage: www.elsevier.com/locate/flora

Anatomical specificities of two paleoendemic flowering desiccation tolerant species of the genus Ramonda (Gesneriaceae)

Tamara Rakić[a,*], Steven Jansen[b], Dragana Rančić[c]

[a] Department of Plant Ecology and Phytogeography, Faculty of Biology, University of Belgrade, 11000 Belgrade, Serbia
[b] Institute of Systematic Botany and Ecology, Ulm University, D-89081 Ulm, Germany
[c] Department of Agrobotany, Faculty of Agriculture, University of Belgrade, 11080 Belgrade, Serbia

ARTICLE INFO

Article history:
Received 29 August 2016
Received in revised form 25 May 2017
Accepted 3 June 2017
Edited by Hermann Heilmeier
Available online 9 June 2017

Keywords:
Contractile stem
Fluorescence microscopy
Lacunar space
Poikilohydric plant
Resurrection plant
Vascular system

ABSTRACT

Ramonda serbica and *R. nathaliae* are known as resurrection flowering plants. Both species are long-living chasmophytes that are physiologically inactive during warm summer periods. Besides numerous known adaptations at the physiological level, it is reasonable to expect that these plant species possess a number of distinctive structural adaptations associated with poikilohydry. Therefore, we analyzed in detail the anatomy of roots, stem and leaves of both species. Plants were collected from their natural habitat or grown from seeds in controlled conditions. Fresh or fixed plant material was sectioned and stained by various histochemical reagents. In addition, vascular tissue was investigated on macerated plant material, and the characteristics of epidermal cells were analyzed on epidermal peelings. Samples were investigated by reflected or transmitted light microscopy, or by scanning electron microscopy. Epidermal cells of the leaves have specific anticlinal beaded thickenings, which could enable maintenance of the epidermis during dehydration and rehydration. Stem vascular tissues form a net-like structure. The shape and arrangement of parenchyma cells appear to support axial contraction. At the base of each adventitious root, a special, thick-walled tissue is observed, which is composed of living cells with pitted walls and probably not involved in long-distance water transport. Overall, various stem and leaf adaptations allow effective water transport through the plant and provide mechanical stability during the relatively fast process of dehydration and rehydration.

1. Introduction

The ability of plants to survive complete dehydration and then accomplish full recovery after a relatively short period of rehydration without structural and physiological damage is called poikilohydry, which is a rare phenomenon among vascular flowering plants. Considering that drought is one of the most serious ecological and economic problems of the modern world, it is important to understand desiccation tolerance mechanisms in plants. Although earlier work has been conducted on the mechanisms involved in desiccation tolerance (Bartels and Salamini, 2001; Vicré et al., 2004; Lüttge et al., 2011; Moore et al., 2013; Farrant et al., 2015), structure-functional aspects associated with poikilohydry remain poorly understood.

From the ca. 300.000 species of flowering plants, only 300 are known to be poikilohydric, of which about 40 species belong to the Eudicots, including plant families such as Cactaceae, Scrophulariaceae, Lamiaceae, Linderniaceae, Plantaginaceae, Gesneriaceae and Myrothamnaceae (Porembski, 2011). In Europe, there are only five eudicotyledonous species known as resurrection plants, all belonging to the Gesneriaceae family: *Ramonda serbica* Panč., *R. nathaliae* Panč. et Petrov., *R. micony* (L.) Rchb., *Haberlea rhodopenis* Friv., and *Jankea heldreichii* (Bioss.) Bioss. These are tertiary relicts and endemics of the Balkan Peninsula, with the exception of *R. micony*, which is found in the Iberian Peninsula. Besides SE Serbia, populations of *Ramonda* species can also be found in southern Balkan areas, with *R. serbica* growing in Albania, Greece, FYR Macedonia, and Montenegro, and *R. nathaliae* occurring in FYR Macedonia, Greece, and Kosovo.

Ramonda serbica and *R. nathaliae* inhabit humid habitats on north exposed slopes of canyons and gorges in rocky outcrops, often sheltered by surrounding shrubs or in the forest understory. Usually, they share their microhabitat with several species of desiccation-tolerant mosses (e.g., *Trichostomum crispulum* Bruch, *Ctenidium molluscum* Mitten) and ferns (*Asplenium ceterach* L., *A. ruta-muraria* L. and *A. trichomanes* L.).

* Corresponding author.
E-mail address: tamaraz@bio.bg.ac.rs (T. Rakić).

http://dx.doi.org/10.1016/j.flora.2017.06.003
0367-2530/

Fig 1. Well hydrated (A) and dehydrated (B) plants of the desiccation tolerant species *Ramonda serbica* (Gesneriaceae) in its natural habitat in SE Serbia. The uprooted plant (C) shows strongly branched and superficial roots.

Although angiosperm resurrection plants share various mechanisms that enable poikilohydry, they also show distinctive structural and physiological differences that have evolved in diverse and highly complex environments. While most angiosperm resurrection plants grow in tropical/subtropical climates of the southern hemisphere, *Ramonda* species from the Balkan area are subject to a high seasonality, with a long, warm and dry summer, and a cold winter with long periods of sub-zero temperatures and a thin snow cover on the steep sides of canyons. Within these climatic conditions, *Ramonda* plants go several times per year through dehydration–rehydration cycles. Usually, during the humid and relatively cold periods of the year (i.e., spring, late autumn, and often winter) both species remain well-hydrated, whereas during the dry and hot summer they survive in a state of physiological inactivity or anabiosis.

Earlier investigations were focused mainly on the physiological, biochemical and molecular aspects of desiccation tolerance (Markovska et al., 1994; Bartels and Salamini, 2001; Bartels, 2005; Moore et al., 2007; Jovanović et al., 2011; Morse et al., 2011; Dinakar and Bartels, 2013; Rakić et al., 2014). So far, only few studies have paid attention to structural features of *R. serbica* and *R. nathaliae*, although it is reasonable to expect that resurrection plants show a number of distinctive structural adaptations at the cell, tissue and organ level that sustain poikilohydry. The morphology and anatomy of some plant organs have been described in various resurrection species: leaves in *Jankaea heldreichii* (Gesneriaceae) (Stevanović and Glisić, 1997) and *Craterostigma plantagineum* (Linderniaceae), *Xerophyta humilis* (Velloziaceae) (Farrant, 2000), leaves, floral structures and stem anatomy in *Myrothamnus flabellifolius* (Myrothamnaceae) (Sherwin et al., 1998; Farrant, 2000; Moore et al., 2006, 2007), leaves and stems of *Reaumuria soongarica* (Tamaricaceae) (Liu et al., 2007) and leaves and roots in the aquatic resurrection plant *Chamaegigas intrepidus* (Linderniaceae) (Schiller et al., 1999; Heilmeier et al., 2002). For *R. serbica* and *R. nathaliae* only leaves have been studied so far (Stevanović and Glisić, 1997; Rascio and La Rocca, 2005).

In adult plants of *R. serbica and R. nathaliae*, the apex of the short aerial part of the stem is covered by 10–15 perennial mesomorphous leaves, organized in a rosette (Fig. 1). Beneath these, the dead marcescent leaves are firmly attached to the stem and protrude above the carpet of mosses that surrounds the stem and covers the soil (Rakić et al., 2009). Although both species grow slowly and are estimated to be long living, their stems usually do not exceed more than three centimetres. It can be presumed that the rehydration efficiency of the stem and, to some extent, the rehydration of the leaves are largely affected by the organization of the stem vascular tissues, which may play a major role during early rehydration.

The aim of the current work is to describe the anatomy of the vegetative plant tissues in *R. serbica* and *R. nathaliae*. Some of the questions that will be addressed include: (1) how are the vascular tissues organized, and (2) how are roots and leaves anatomically integrated via vascular bundles to tolerate dehydration, while enabling at the same time fast and efficient water uptake during rehydration.

2. Material and methods

One-year-old plants and adult plants were collected from their natural habitat in the Jelasnica gorge in SE Serbia. In addition, young plantlets were grown from seeds in a sterile culture medium (Murashige and Skoog, 1962) for three months.

The whole plant morphology and sections of larger areas were observed using a stereomicroscope (Nikon SMZ 18).

Transverse sections were taken from one-month- and three-months-old plantlets, one-year-old plants, and adult plants. A series of transverse and longitudinal sections, 8–10 μm thick, were obtained from the entire body of the stem, leaves and roots. Plants were sectioned fresh or fixed in FAA and 50% ethanol prior to preparation for a standard paraffin method (Ruzin, 1999).

Fresh plant material was hand sectioned with a razor blade or 40 μm thick sections were cut with a cryo-microtome (Leica CM 1850) at −21 °C, and observed by epi-fluorescence microscopy to detect autofluorescence, or stained with toluidine blue (O'Brien et al., 1964). Additional stains included phloroglucinol-HCl to detect lignified cell walls (Jensen, 1962), Sudan IV for lipids (Pearse, 1980), Lugol to visualise starch (Johansen, 1940), and ferric trichloride to identify phenolic compounds (Johansen, 1940). Paraffin sections were double stained in safranin (1%, w/v in 50% ethanol) and alcian blue (1% w/v, aqueous). In addition, root, stem and leaf tissue was macerated in a mixture of concentrated glacial acetic acid and 30% hydrogen peroxide (1:1 v/v) at 60 °C, until the samples turned white (1–5 days). The macerated cells were stained with safranin. Vessel diameters were measured on transverse sections at the widest part of the vessel, excluding the cell wall. The length of vessel elements was measured including their tails. Microslides were examined and photographed using a Leica DMLS light microscope equipped with a Leica DFC295 digital camera.

In order to observe water absorption and long-distance water transport, dry plants were treated separately with 5(6)-Carboxyfluorescein (Grignon et al., 1989; Viola et al., 2001) and Eosin Y (Baum et al., 2000) as fluorescent markers of phloem and xylem transport, respectively. The stem sections were obtained 24 h after the beginning of rehydration and observed by epi-fluorescence microscopy.

To test for autofluorescence and dye fluorescence an epi-fluorescence Olympus BX51 microscope equipped with an HBO 50 W mercury vapour lamp with wide-band BV excitation filter (excitation filter BP400-440, dichroic beam splitter DM455 and barrier filter BA475) and wide band Blue excitation filter (excitation filter BP460-490, beam splitter DM500, barrier filter BA520IF) were used. All anatomical parameters were measured using the software programme Leica Q Win (Leica Microsystems, Germany).

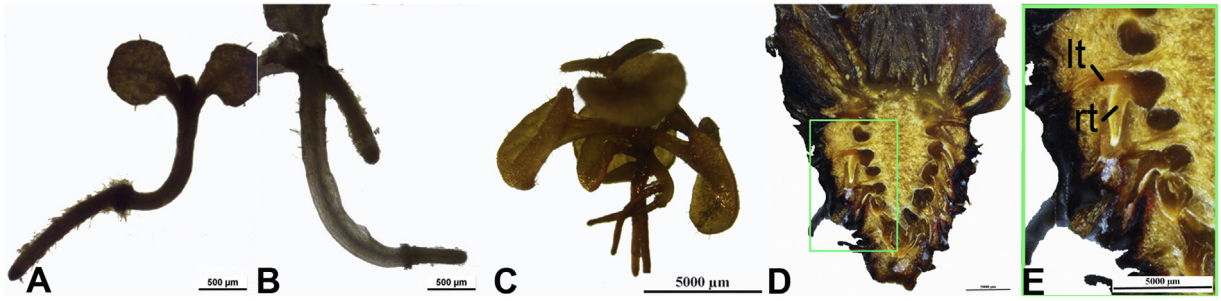

Fig. 2. Developmental stages of *Ramonda serbica* showing root and shoot details. One-month-old plantlet (A), three-months-old plantlet with the first nodal root (B), one-year-old plant with nodal roots (C), the longitudinal cross section of the stem in an adult plant (D) and detailed view with root trace (rt) and leaf petiole base (lt) arising close to each other from the axial vascular bundle (E).

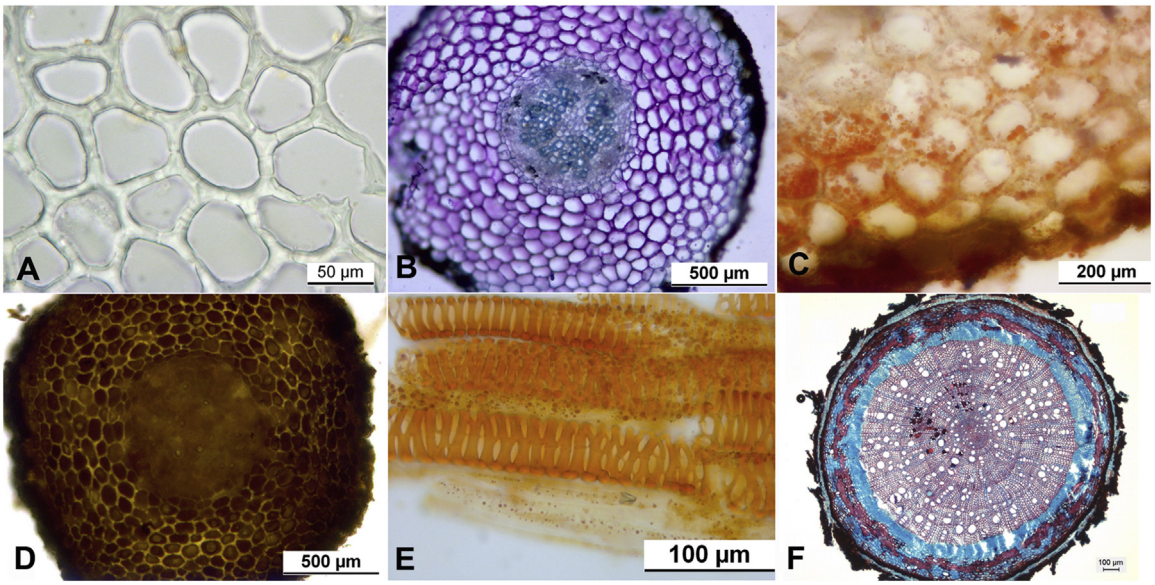

Fig. 3. Unstained parenchyma cells in root cortex (A); Transverse section through the primary root stained with toluidine blue (B); The orange colour in outer parenchyma cells within root cortex indicates presence of lipid droplets, based on staining with Sudan (C); Brown colour indicating the presence of phenolic compounds stained with $FeCl_3$ (D); Ornamentation of a xylem vessel in a macerated root sample stained with safranin (E) and secondary root structure stained with safranin and alcian blue (F). (For interpretation of the references to colour in this figure legend, the reader is referred to the web version of this article.)

In addition, some details regarding leaf and stem anatomy, xylem elements and vascular sclerenchyma were analyzed using a JEOL JSM-6460LV scanning electron microscope.

3. Results

3.1. Root morphology and anatomy

The young, one-month-old seedlings possess only a primary root (Fig. 2A). At an early stage of plant development, lateral roots as well as adventitious roots arising from the stem node can be observed (Fig. 2B, C). During later developmental stages more nodal roots occur and, on the longitudinal section of the adult plant stem, numerous, thin adventitious roots arise from each node (Fig. 2D, E). From the same node from which a root appears, a leaf petiole arises, which grows in the opposite direction to the root.

The cortex of the primary root, which comprises the largest volume of the root, consists of three regions. Two or three layers of tangentially elongated and suberized parenchyma cells form the outer protective exodermis. The middle region is multi-layered, with cells elongated in the longitudinal direction, and a third, inner endodermis is composed of an uneven row of smaller cells of more or less spherical shape. The cortex cells have unusually thick walls (4.6 ± 0.97 µm, mean value ± SD; Fig. 3A), which are stained violet in presence of toluidine blue, a colour that is typical of primary cell walls rich in pectins and cellulose (Fig. 3B). Transverse sections stained by lugol indicate the absence of starch storage in the cortex. On the other hand, histochemical staining shows the presence of lipid droplets in the outer cortical cells (Fig. 3C) and the presence of phenolic compounds (Fig. 3D). In roots showing primary growth, the vessel diameter including the vessel wall is 12.7 ± 1.6 µm and 24.4 ± 3.7 µm in *R. serbica* and *R. nathaliae*, respectively, and the vessel element length is 110.9 ± 61.2 µm and 105.7 ± 36.9 µm, respectively. The thickness of the secondary cell wall is 2.7 ± 0.8 µm in *R. serbica* and 3.1 ± 0.6 µm in *R. nathaliae*. Tracheary elements with both scalariform and reticulate patterns of thickening are present in the xylem (Fig. 3E).

Although most roots that spread from the stem have a typical primary structure, secondary thickening can also be seen in some roots (Fig. 3F).

3.2. Stem morphology and anatomy

The underground part constitutes the largest portion of the stem, from which the strongly branched roots extend into the shallow soil (Fig. 1C). The stem of young plants that are about 1–2 years old is straight, with no wrinkled surface. Longitudinal and transverse sections of the stem and peduncle show regularly positioned,

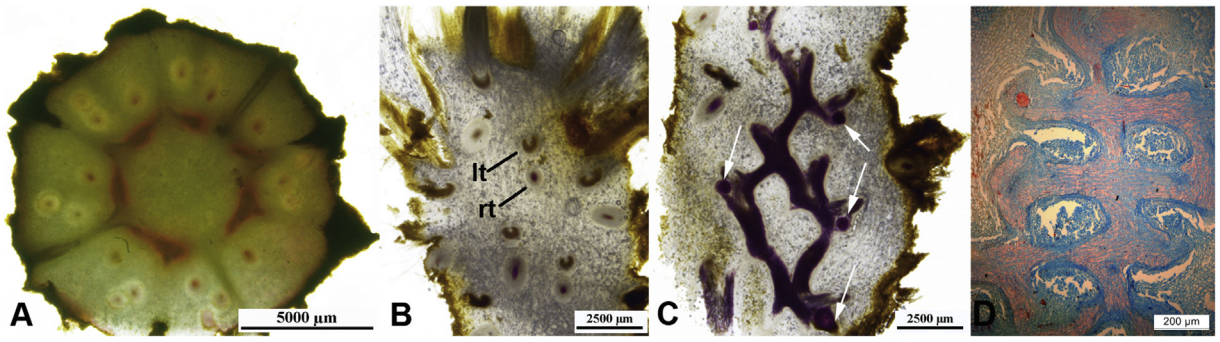

Fig. 4. Hand cross-sections of a stem stained with phloroglucinol-HCl: Transverse section of the stem (A), longitudinal section of the stem with pairs of leaf (lt) and root traces (rt) along the stem (B), longitudinal section at the level of axial vascular bundles with clusters of vascular sclerenchyma arrowed (C). Longitudinal section, double stained with safranin and alcian blue (D). (For interpretation of the references to colour in this figure legend, the reader is referred to the web version of this article.)

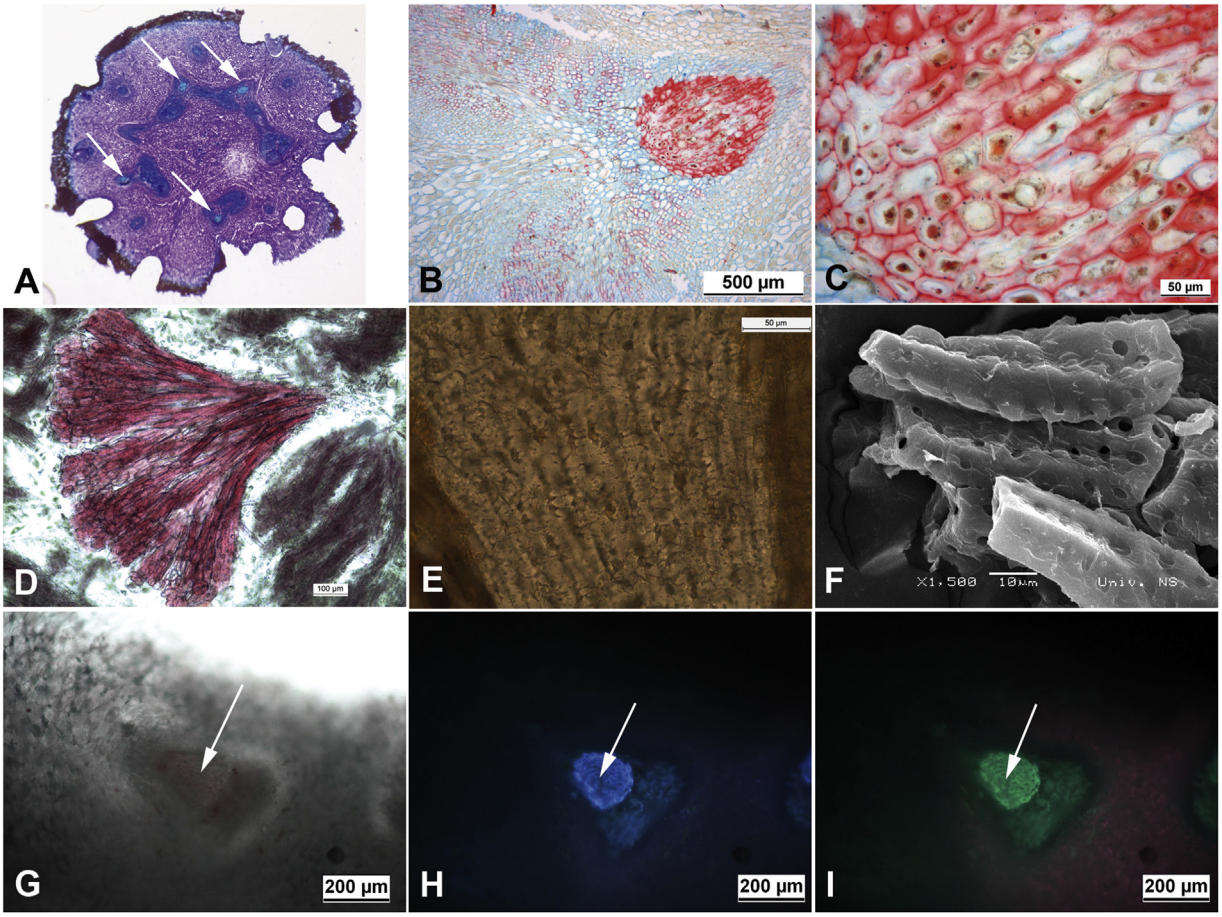

Fig. 5. Vascular sclerenchyma visible on transverse sections of the stem: stained intense green with toluidine blue (A) or stained intense red with a double safranin-alcian blue staining (B, C). Slightly pressed cluster of vascular sclerenchyma tissue observed in macerated stem tissue (D). Unstained, longitudinal section through vascular sclerenchyma tissue (E) and SEM micrograph of individual cells (F). Vascular sclerenchyma in unstained transverse section observed with a light microscope (G). Autofluorescence of lignin in vascular sclerenchyma cell walls under BV filter (H) and Blue excitation filter (I), arrowed. (For interpretation of the references to colour in this figure legend, the reader is referred to the web version of this article.)

individual collateral vascular bundles and therefore a typical primary stem anatomy. Over the years, as the stem grows, it contracts axially. In older plants, the stem is mostly up to 3 cm long and has a noticeably rugged outer surface (Fig. 2D). The surface of the shoot apex and leaf primordia are covered densely with long hairs composed of some living cells at their base, whereas the upper part is made of dead cells (Fig. 2D).

Transverse cross-sections show the presence of a periderm on the surface, a relatively wide cortex zone and a central vascular cylinder (Fig. 4A). The outer cortex consists of thin-walled parenchyma cells and single vascular bundles showing leaf and root traces. Although the age of the plant specimens was estimated to be more than five to ten years, the vascular bundles run separately and extend radially during the secondary growth, without connecting laterally and thus never form a continuous ring. Adventitious roots originate from the vascular central ring of the stem and pass through the cortical region during their development. These lateral roots are visible in both longitudinal and transverse sections, almost over the entire length of the stem, and are most abundant in the lower part of the stem. In the longitudinal paradermal sections,

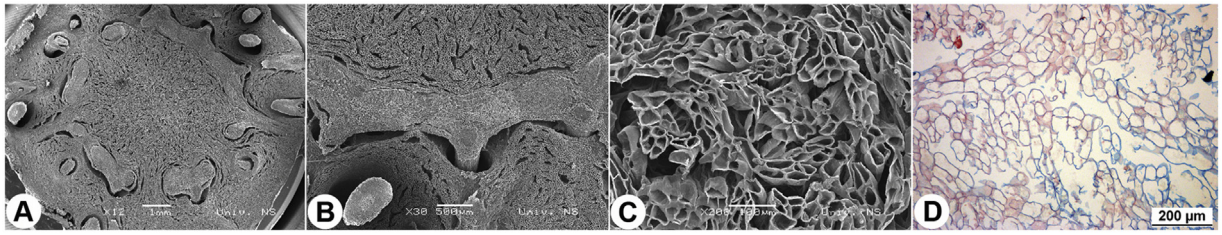

Fig. 6. SEM micrographs of a stem transverse section (A, B) and pith parenchyma cells observed with SEM (C) and light microscopy (D).

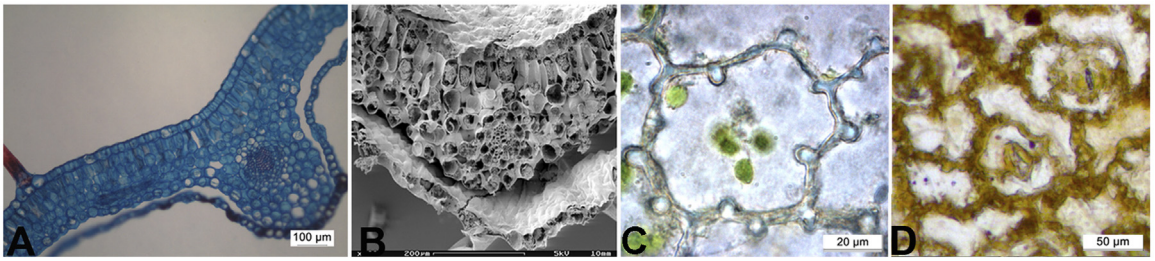

Fig. 7. Leaf cross-section stained with safranin and alcian blue and observed with a light microscope (A) and with SEM (B). Light microscopy of anticlinal epidermal cell walls in hydrated (C) and dehydrated leaf (D). (For interpretation of the references to colour in this figure legend, the reader is referred to the web version of this article.)

only root and leaf petiole traces can be observed, and are always present in pairs (Fig. 4B).

Transverse sections of the stem illustrate the anatomical variation along the short stem axis, which derives from a specific organization of the vascular tissue at different stem levels. A series of longitudinal sections through the stem of both *Ramonda* species reveals the net-like organization of vascular tissues that is formed by connection between neighbouring, sinuous axial vascular bundles (Fig. 4C, D). As a result, some of the longitudinal sections reveal continuous strands of vascular bundles, whereas others show separate vascular bundles in a vertical sequence (Fig. 4B–D). The vascular network of the stem vascular ring is connected directly to the leaf and to the root traces at nodes – one vascular trace diverges to supply both the leaf and the root trace (Fig. 4C). Vessel elements in *R. serbica* and *R. nathaliae* are 100.0 ± 36.6 μm and 66.0 ± 15.0 μm long and 12.8 ± 2.8 μm and 12.0 ± 2.1 μm wide in their outer diameter, respectively. The thickness of the secondary cell wall is 2.0 ± 0.3 μm in *R. serbica* and 2.2 ± 0.5 μm in *R. nathaliae*. Pitting in xylem is reticulate (Fig. 3E).

Clusters of specific tissue are associated with the stem vascular bundles. Clusters are composed of closely packed thick-walled cells with pitted walls, which form distinct compact structures that have a patchy, but very regular distribution within the vascular network (Fig. 5A–C). This tissue is present only at nodes, always at the base of the root, but never at the base of the leaf trace (Fig. 4C). It can be found even in the zone next to the apical meristem. The cells are thick-walled, elongated longitudinally, always shorter at the base of the compact cylindrical structure than at its upper part, and are characterized by a pitted-like structure visible in their outer surface (Fig. 5D–F). In *R. serbica*, the short basal cells are 48.0 ± 7.6 μm long and 23.4 ± 2.9 μm wide in their outer diameter, whereas the long cells are 109.9 ± 31.1 μm long and 15.0 ± 2.4 μm wide. In *R. nathaliae* the length and width of short cells are 43.9 ± 7.2 μm and 17.2 ± 2.1 μm, whereas those of the long ones are 173.3 ± 26.5 μm and 16.8 ± 2.5 μm. The average diameter of the cell lumen in both species is 12.9 ± 5.6 μm. Most frequently, the cell lumen is filled with dense, red-brown substances. At higher magnification, their inner cell wall surface is seen to be undulated and, despite much reduced cell volume, these cells are alive, possessing a cytoplasm with a nucleus (Fig. 5D). Their cell walls are 9.3 ± 1.8 μm thick, much thicker than those of ordinary stem xylem vessels. The cell walls of this unusual type of lignified cell stain similarly as xylem, but with a different tone: they are more greenish than blue when stained with toluidine blue (Fig. 5A), and crimson red when stained with safranin or phloroglucinol (Fig. 5B). These cells show a strong autofluorescence under an epifluorescence microscope (Fig. 5G–I). The stem and leaf cross-sections were analyzed after plant rehydration, 24 h after the treatment. In stem sections, these lignified cells remained unstained with 5,6-Carboxyfluoresceine (phloem tracer). Only the outer cells became stained with Eosin Y (xylem tracer), whereas the inner ones remained unstained, showing only autofluorescence (not shown). The staining of the outer layer of these lignified cells is probably a consequence of passive dye diffusion from the surrounding parenchyma cells that absorb water with diluted dye. The stem pith consists of thin-walled parenchyma with an average transverse diameter of 104.3 ± 16.3 μm, length of 136.5 ± 40.2 μm, and longitudinal width of 56.3 ± 21.4 μm. The parenchyma cells have a variable shape and size, there is no clear alignment of these cells in a transverse or longitudinal plane, and the intercellular spaces are far less spacious in well hydrated plants than in desiccated ones (Fig. 6A–D). In a longitudinal section the cortical parenchyma cells are larger than the pith cells, especially those lying in-between two branches of vascular tissue. The layers of parenchyma cells that are directly associated with the vascular bundles are strikingly compressed (Fig. 4D). In dried plants, wide, regular gaps occur between the vascular bundles and the parenchymal tissue (Fig. 6A, B).

3.3. *Leaf anatomy*

The leaf blade is bifacial and the palisade cells are very short and arranged in one or two layers; the spongy tissue consists of few cell layers (Fig. 7A, B). Leaves are hypostomatic in *R. serbica* and amphistomatic in *R. nathaliae*. Anisocytic stomata are aligned with epidermal cells in both species. The dimensions of stomata and their densities were previously described and discussed by Rakić et al. (2015).

Epidermal cells, viewed from the surface, are more or less polygonal or undulated with very conspicuous beaded cell wall thickenings, which extend as short columns and are more prominent in the lower epidermis (Fig. 7C, D). The latter is loosely attached to the mesophyll of the leaf between major leaf veins and

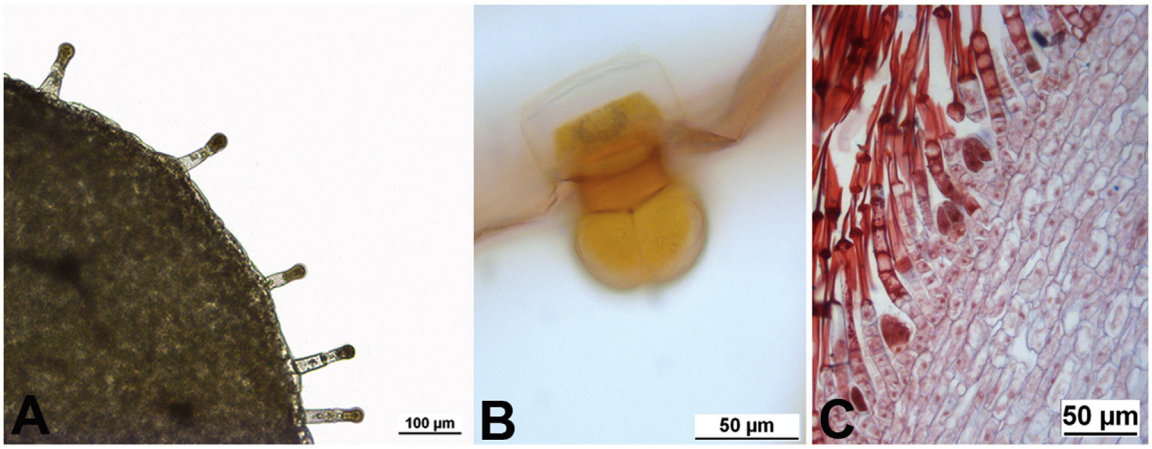

Fig. 8. Two types of glandular trichomes present on the leaf surface of a three-month-old plantlet (A, B). Longitudinal section of the shoot apex showing leaf petioles, densely covered with long, uniseriate hairs and glandular hairs (C).

can therefore be very easily peeled off from the main body of the leaf (Fig. 7A, B). This is characteristic of both fully developed leaves and young leaves during earlier developmental stages. The epidermal detachment is most evident in *R. serbica*. Vessels in the midribs and leaf petiole are with helical thickenings and are 23.9 ± 6.4 μm wide (including vessel walls). The vessel elements in *R. serbica* and in *R. nathaliae* are 280.0 ± 101.8 μm and 242.1 ± 106.4 μm long, respectively.

The indumentum on leaves and leaf petioles is composed of multicellular, unbranched trichomes (Fig. 8A–C), which are especially numerous on the lower epidermis. The stalked glandular trichomes are randomly scattered over the leaf surface. Some glandular hairs have a longer stalk with two apical glandular cells (Fig. 8A), whereas others have a short stalk and a head divided by vertical walls into four cells (Fig. 8B). The basal part of the leaf petiole is covered by an extremely dense indumentum of linear, non-glandular trichomes (Fig. 8C).

4. Discussion

One of the striking morphological features of the resurrection chasmophytic plants *Ramonda serbica* and *R. nathaliae* is the very short stem, which is mainly located below- ground in adult plants and not longer than 3 cm. From most of its conspicuously rugged surface, various thin and highly branched roots grow. These fine roots strongly permeate the shallow organo-mineral substrate and in the presence of vesicular-arbuscular mycorrhizal fungi (Rakić et al., 2009, 2013) are highly effective in absorbing water and nutrients from the soil. In both species, the stem shows nonspecific secondary growth characterized by radial extension of individual vascular bundles, which do not join laterally during plant growth and ageing. Axial vascular bundles show a net-like organization within the stem and are sinuously folded, suggesting that there is a permanent and vertical stem contraction. Moreover, the strikingly pressed layers of parenchyma cells that rest directly against the vascular bundles and the unequally oriented pith parenchyma cells point to stem compression. The extremely similar, net-like organization, as well as the permanent vertical contraction of the stem, has only been described in detail in the megaherb *Pleurophyllum hookeri* Buchanan from the Macquarie Island (Briggs et al., 2006). At the same position near the nodes, the vascular network in *Ramonda* plants diverges to supply both the leaf and the root trace. This kind of organization of the stem vascular tissue and highly integrated root–leaf vascular system could be beneficial in water absorption and a very efficient distribution of water between the roots, stem and leaves. A specific criss-cross organization of axial bundles may also offer high mechanical stability of the stem during volume changes provoked by fluctuations in its water content due to numerous dehydrations and rehydrations to which plants are exposed repeatedly during their life span.

Clusters of thick-walled cells with circular pits have a patchy but regular position within the stem, on the outer side of the vascular network, and occur exclusively at the basal part of adventitious roots. Upon maturation these cells are as long as vessel elements (in *R. serbica*) and even three times as long as vessel elements (in *R. nathaliae*). The difference in the size of cells within one patch, which varies from two to almost four times, could be explained by differences in their ageing, and therefore different effects of environmental conditions on their growth and development. Their highly lignified and pitted cell walls, apparently thicker than vessel walls, and the patchy occurrence of this specific tissue along the stem, even next to the apical meristem, indicate that it differentiates rather early during stem development relative to xylem. The histochemical staining and autofluorescence observations show that the chemical composition of their cell walls and that of the xylem differs. This tissue seems to be similar to what was previously described in the stem of the monocot species *Eriophorum vaginatum* L. (Cyperaceae) (Cholewa and Griffth, 2004). Although Cholewa and Griffth (2004) described it as "vascular sclerenchyma" and proposed it to have the ability to aid in xylem and phloem long-distance transport, we could not confirm a xylem or phloem link because fluorescent dyes were not observed within this tissue 24 h after re-watering. However, it is possible that it retains water for some time even after the vessel elements lost the water column upon desiccation, and that it offers higher strength to the stem.

Whereas connectivity exists between all stem tissues in well hydrated plants, dried stems show gaps between vascular bundles and the surrounding parenchyma tissue. Difference in hardness and elasticity between thin-walled parenchyma and thick-walled vascular tissues and therefore in the level of volume reduction lead to their separation. The several layers of collapsible parenchyma tissue, detected along the vascular bundles, facilitate a volume change in parenchyma tissue provoked by plant desiccation and rewatering. Although gaps might represent spots of potential pathogen attack to plant tissues, intensive histochemical black staining verifies the presence of large amounts of phenolic compounds, which may have antimicrobial properties. The high amounts of phenolic acids were found in the *Ramonda* leaves, with the most abundant ones being protocatechuic, p-hydroxybenzoic and chlorogenic acids (Sgherri et al., 2004), which are known to have an antibacte-

rial activity (Tuncel and Nergiz, 1993; Taguri et al., 2006; Landete et al., 2008; Campos et al., 2009; Cueva et al., 2010; Merkl et al., 2010; Xia et al., 2010).

The anatomy of xylem is known to be correlated closely with the plant habit and its habitat (Carlquist, 2008). In the case of vascular resurrection plants, it is also finely attuned to the efficient water economy within the plant during repeated dehydration–rehydration cycles. The vessel diameter in root, stem and leaves in both *Ramonda* species are, on average, less than 25 μm, which is similar to the value reported for the stem vessels in the resurrection plant *Myrothamnus flabellifolius* Welw. (Myrothamnaceae), whose stem xylem vessels are ca. 14 μm in diameter (Sherwin et al., 1998). The narrow vessels in *Ramonda* can be suggested to avoid embolism resistance, which would be strengthened by the presence of surface active lipids in xylem sap (Wagner et al., 2000; Schenk et al., 2017).

In contrast to the shorter, reticulate xylem elements in the stem, the helical xylem elements in the leaf midrib and in the leaf petiole are relatively long and act like strings, without limiting the leaf movements. However, despite their spiral support and elasticity, the helical structure may endure contractions to a certain degree and thus limits and directs the shrinking process of the leaf during desiccation, as shown in the aquatic resurrection plant *Chamaegigas intrepidus* Dinter ex Heil (Schiller et al., 1999).

The upper and the lower leaf epidermis in both plant species is characterized by distinct cell wall thickenings with an indented appearance of their anticlinal cell walls, as previously reported for *R. nathaliae* by Rascio and La Rocca (2005). There is remarkable similarity between the regularly beaded appearance of the epidermal cell walls in the two *Ramonda* species and the sward-like formations (resembling "jigsaw pieces") described in epidermal cell walls in flower petals of *Petunia hybrida* (Lysenko and Varduny, 2013). The authors proposed a potential relationship between an anthocyanin-dependent photochemical process and the cell wall ingrowths (Lysenko and Varduny, 2013), as well as their possible role in cytoplasm sequestration (Lysenko et al., 2016). However, a different functional role is likely in resurrection plants of *Ramonda*, which may experience significant changes in their leaf surface area and leaf folding (Rakić et al., 2015) during dehydration–rehydration cycles. The localized wall depositions could provide strong mechanical support to the epidermis and enable maintenance of its integrity and that of the entire leaf during water loss, and ensure proper restoration of its morphology during subsequent rehydration.

Although the more prominent indented appearance of anticlinal cell walls was expected in dehydrated epidermal cells, it was not observed. Therefore, it could be assumed that a decrease in epidermal surface occurs at the expense of change in cell wall composition and its inner architecture, as reported in leaves of *Myrothamnus flabellifolius* (Moore et al., 2006), giving it flexibility and enabling changes in the size of the protoplast and the entire mesophyll.

Another interesting structural feature of the leaf, that is clearly visible in all sections, is detachment of the lower epidermis from the spongy parenchyma. Its loose connection to spongy tissue may be demonstrated by its easy peeling from the largest part of the lamina between the largest nerves, those of the 1° and the 2° vein order, using a forceps. This space between adaxial epidermis and spongy parenchyma or "pockets" are more noticeable in leaves of *R. serbica* and were previously documented in *R. nathaliae* (Rascio and La Rocca, 2005). When the dry and folded leaves, which have an abaxial surface with stomata oriented outward, come in contact with water from rain, small amounts of water might arrive in the pockets beneath epidermal cells and could then be pulled by capillary forces to mesophyll cells and support fast recovery. Nevertheless, the presence of a "detached" lower epidermis can also be related to changes in leaf dimensions during dehydration–rehydration cycles. The partial detachment of a lower epidermis from mesophyll could enable their independent movement during changes in leaf rehydration and avoidance of mechanical disruption of mesophyll and epidermal cells.

5. Conclusions

The sinuously folded axial vascular bundles, the shape of the elongated pith parenchyma cells, and the number of strikingly pressed layers of parenchyma cells that are positioned next to the vascular bundles are characteristic stem features in *R. serbica* and *R. nathaliae* that may enable stem contraction. The short stem, with the specific vascular tissue organization, is connected to numerous and thin adventitious roots that arise from each stem node, and is in immediate proximity to root and leaf traces. This vascular tissue organization may contribute to efficient water transport, which would be important for fast rehydration.

Various structural adaptations, such as pitting of the stem and leaf xylem elements, organization of stem vascular tissues, loose connection of lower leaf epidermis to mesophyll, and specific thickenings in anticlinal cell walls of epidermal cells, allow direct volume and shape changes and might offer high mechanical stability to the stem and leaves, and effective re-establishment of water uptake during rehydration. However, the function of specific "vascular sclerenchyma" tissue observed in the stem of both *Ramonda* species remains unclear.

Acknowledgement

This work was supported by the Ministry of Education, Science and Technological Development of Serbia (Grants No. 173030 and TR31005).

References

Bartels, D., Salamini, F., 2001. Desiccation tolerance in the resurrection plant *Craterostigma plantagineum*: A contribution to the study of drought tolerance at the molecular level. Plant Phys. 127, 1346–1353.
Bartels, D., 2005. Desiccation tolerance studied in the resurrection plant *Craterostigma plantagineum*. Integr. Comp. Biol. 45, 696–701.
Baum, S.F., Tran, P.N., Silk, W.K., 2000. Effects of salinity on xylem structure and water use in growing leaves of sorghum. New Phytol. 146, 119–127.
Briggs, C.L., Selkirk, P.M., Bergstrom, B.M., 2006. Facing the furious fifties: the contractile stem of the subantarctic megaherb *Pleurophyllum hookeri*. N. Z. J. Bot. 44, 187–197.
Campos, F.M., Couto, J.A., Figuereido, A.R., Toth, I.V., Rangel, A.O.S.S., Hogg, T.A., 2009. Cell membrane damage induced by phenolic acids on wine lactic acids bacteria. Int. J. Food Microbiol. 135, 144–151.
Carlquist, S., 2008. Monocot xylem revisited New information, new paradigms. Bot. Rev. 78, 87–153.
Cholewa, E., Griffth, M., 2004. The unusual vascular structure of the corm of *Eriophorum vaginatum*: implications for efficient retranslocation of nutrients. J. Exp. Bot. 55, 731–741.
Cueva, C., Moreno-Arribas, M.V., Martinez-Alvarez, P.J., Bills, G., Vicente, M.F., Basilio, A., Rivas, Lopez, Requena, C., Rodríguez, T., Bartolomé, J.M., 2010. Antimicrobial activity of phenolic acids against commensal, probiotic and pathogenic bacteria. Res. Microbiol. 16, 372–382.
Dinakar, C., Bartels, D., 2013. Desiccation tolerance in resurrection plants: new insights from transcriptome, proteome and metabolome analysis. Front. Plant Sci. 4, 482.
Farrant, J.M., Cooper, K., Hilgart, A., Abdalla, K.O., Bentley, J., Thomson, J.A., Dace, H.J.W., Peton, N., Mundree, S.G., Rafudeen, M.S., 2015. A molecular physiological review of vegetative desiccation tolerance in the resurrection plant *Xerophyta viscosa* (Baker). Planta 242, 407–426.
Farrant, J.M., 2000. A comparison of mechanisms of desiccation tolerance among three angiosperm resurrection plant species. Plant Ecol. 151, 29–39.
Grignon, N., Touraine, B., Durand, M., 1989. 6(5)Carboxyfluorescein as a tracer of phloem sap translocation. Am. J. Bot. 76, 871–877.
Heilmeier, H., Wolf, R., Wacker, R., Woitke, M., Hartung, W., 2002. Observations on the anatomy of hydrated and dehydrated roots of *Chamaegigas intrepidus* Dinter. Dinteria 27, 1–12.
Jensen, W.A., 1962. Botanical Histochemistry: Principles and Practices. WH Freeman and Co., San Francisco.
Johansen, D.A., 1940. Plant Microtechnique. McGraw-Hill Book Comany, New York, London.

Jovanović, Ž., Rakić, T., Stevanović, B., Radović, S., 2011. Characterization of oxidative and antioxidative events during dehydration and rehydration of resurrection plant *Ramonda nathaliae*. Plant Growth Regul. 64, 231–240.
Lüttge, U., Beck, E., Bartels, D., 2011. Plant Desiccation Tolerance. Springer-Verlag, Berlin.
Landete, J.M., Curiel, J.A., Rodriguez, H., Rivas, B., Muñoz, R., 2008. Study of the inhibitory activity of phenolic compounds found in olive products and their degradation by *Lactobacillus plantarum* strains. Food Chem. 107, 320–326.
Liu, Y.B., Wang, G., Liu, J., Zhao, X., Tan, H.J., Li, X.R., 2007. Anatomical, morphological and metabolic acclimation in the resurrection plant *Reaumuria soongorica* during dehydration and rehydration. J. Arid. Environ. 70, 183–194.
Lysenko, V., Varduny, T., 2013. Anthocyanin-dependent anoxygenic photosynthesis in coloured flower petals? Sci. Rep., 3.
Lysenko, V., Fedorenko, G., Fedorenko, A., Kirichenko, E., Logvinov, A., Varduny, T., 2016. Targeting of organelles into vacuoles and ultrastructure of flower petal epidermis of *Petunia hybrida*. Braz. J. Bot. 39, 327–336.
Markovska, Y.K., Tsonev, T.D., Kimenov, G.P., Tutekova, A.A., 1994. Physiological changes in higher poikilohydric plants - *Haberlea rhodopensis* Friv. and *Ramonda serbica* Panč. during drought and rewatering at different light regimes. J. Plant Phys. 144, 100–108.
Merkl, R., Hrádková, I., Filip, V., Šmidrkal, J., 2010. Antimicrobial and antioxidant properties of phenolic acids alkyl esters. Czech J. Food Sci. 28, 275–279.
Moore, J.P., Nguema-Ona, E., Chevalier, L., Lindsey, G.G., Brandt, W.F., Lerouge, P., Farrant, J.M., Driouich, A., 2006. Response of the leaf cell wall to desiccation in the resurrection plant *Myrothamnus flabellifolius*. Plant Phys. 141, 651–662.
Moore, J.P., Lindsey, G.G., Farrant, J.M., Brandt, W.F., 2007. An overview of the biology of the desiccation-tolerant resurrection plant *Myrothamnus flabellifolia*. Ann. Bot. 99, 211–217.
Moore, J.P., Nguema-Ona, E.E., Vicré-Gibouin, M., Sørensen, I., Willats, W.G.T., Driouich, A., Farrant, J.M., 2013. Arabinose-rich polymers as an evolutionary strategy to plasticize resurrection plant cell walls against desiccation. Planta 237, 739–754.
Morse, M., Rafudeen, M.S., Farrant, J.M., 2011. An overview of the current understanding of desiccation tolerance in the vegetative tissues of higher plants. Adv. Bot. Res. 57, 319–347.
Murashige, T., Skoog, F., 1962. A revised medium for rapid growth and bio assays with tobacco tissue cultures. Physiol. Plant. 15, 473–497.
O'Brien, T.P., Feder, N., McCully, M.E., 1964. Polychromatic staining of plant cell walls by toluidine blue O. Protoplasma 59, 368–373.
Pearse, A.G.E., 1980. Histochemistry Theoretical and Applied, fourth ed. Longman Group Limited, London.
Porembski, S., 2011. Evolution, diversity and habitats of poikilohydrous vascular plants. In: Lüttge, U., Beck, E., Bartels, D. (Eds.), Plant Desiccation Tolerance. Springer-Verlag, Berlin, pp. 139–156.
Rakić, T., Quartacci, M.F., Cardelli, R., Navari-Izzo, F., Stevanović, B., 2009. Soil properties and their effects on water and mineral status of resurrection *Ramonda serbica*. Plant Ecol. 203, 13–21.
Rakić, T., Ilijević, K., Lazarević, M., Gržetić, I., Stevanović, V., Stevanović, B., 2013. The resurrection flowering plant *Ramonda nathaliae* on serpentine soil —meeting an extreme challenge in adaptive ability: mineral element composition in soil and in plant. Flora 208, 618–625.
Rakić, T., Lazarević, M., Jovanović, Ž., Radović, S., Siljak-Yakovlev, S., Stevanović, B., Stevanović, V., 2014. Resurrection plants of the genus *Ramonda*: prospective survival strategies —unlock further capacity of adaptation, or embark on the path of evolution? Front. Plant Sci. 4, 550.
Rakić, T., Gajić, G., Lazarević, M., Stevanović, B., 2015. Effects of different light intensities CO_2 concentrations, temperatures and drought stress on photosynthetic activity in two paleoendemic resurrection plant species *Ramonda serbica* and *R. nathaliae*. Environ. Exp. Bot. 109, 63–72.
Rascio, N., La Rocca, N., 2005. Resurrection plants: the puzzle of surviving extreme vegetative desiccation. Crit. Rev. Plant Sci. 24, 209–225.
Ruzin, S.E., 1999. Plant Microtechnique and Microscopy. Oxford University Press, New York, USA.
Schenk, H.J., Espino, S., Romo, D.M., Nima, N., Do, A.Y.T., Michaud, J.M., Papahadjopoulos-Sternberg, B., Yang, J., Zuo, Y.Y., Steppe, K., Jansen, S., 2017. Xylem surfactants introduce a new element to the cohesion-tension theory. Plant Physiol. 173, 1177–1196.
Schiller, P., Wolf, R., Hartung, W., 1999. A scanning electron microscopical study of hydrated and desiccated submerged leaves of the aquatic resurrection plant *Chamaegigas intrepidus*. Flora (Jena) 194, 97–102.
Sgherri, C., Stevanovic, B., Navari-Izzo, F., 2004. Role of phenolics in the antioxidative status of the resurrection plant *Ramonda serbica* during dehydration and rehydration. Physiol. Plant. 122, 478–485.
Sherwin, H.W., Pammenter, N.W., February, E.D., van der Willigen, C., Farrant, J.M., 1998. Xylem hydraulic characteristic, water relation and wood anatomy of the resurrection plant *Myrothamnus flabellifolius*. Ann. Bot. 81, 567–575.
Stevanović, B., Glisić, O., 1997. Eco-anatomical differences between Balkan endemo-relict species of Gesneriaceae. Bocconea 5, 661–665.
Taguri, T., Tanaka, T., Kouno, I., 2006. Antibacterial spectrum of plant polyphenols and extracts depending upon hydroxyphenyl structure. Biol. Pharm. Bull. 29, 2226–2235.
Tuncel, G., Nergiz, C., 1993. Antimicrobial effect of some olive phenols in a laboratory medium. Lett. Appl. Microbiol. 17, 300–302.
Vicré, M., Lerouxel, O., Farrant, J., Lerouge, P., Driouich, A., 2004. Composition and desiccation-induced alterations of the cell wall in the resurrection plant *Craterostigma wilmsii*. Physiol. Plant. 120, 229–239.
Viola, R., Roberts, A.G., Haupt, S., Gazzani, S., Hancock, R.D., Marmiroli, N., Machray, G.C., Oparka, K.J., 2001. Tuberization in potato involves a switch from apoplastic to symplastic phloem unloading. Plant Cell 13, 385–398.
Wagner, H.J., Schneider, H., Mimietz, S., Wistuba, N., Rokitta, M., Krohne, G., Haase, A., Zimmermann, U., 2000. Xylem conduits of a resurrection plant contain a unique lipid lining and refill following a distinct pattern after desiccation. New Phytol. 148, 239–255.
Xia, D., Wu, Z., Shi, J., Yang, Q., Zhang, Y., 2010. Phenolic compounds from the edible seeds extract of Chinese Mei (*Prunus mume* Sieb et Zucc) and their antimicrobial activity. LWT Food Sci. Technol. 44, 347–349.